

Surface Wave Assisted Self-Assembly of Multidomain Magnetic Structures

A. Snezhko, I. S. Aranson, and W.-K. Kwok

Materials Science Division, Argonne National Laboratory, 9700 South Cass Avenue, Argonne, Illinois 60439, USA

(Received 31 May 2005; published 21 February 2006)

An ensemble of magnetic microparticles at the liquid surface displays novel snakelike self-assembled structures induced by an alternating magnetic field. We demonstrate that these structures are directly related to surface waves in the liquid generated by the collective response of magnetic microparticles to the alternating magnetic field. The segments of the “snake” exhibit long-range antiferromagnetic ordering, while each segment is composed of ferromagnetically aligned chains of microparticles. The structures exhibit magnetic hysteretic behavior with respect to an external in-plane magnetic field and logarithmic relaxation of the remanent magnetic moment.

DOI: [10.1103/PhysRevLett.96.078701](https://doi.org/10.1103/PhysRevLett.96.078701)

PACS numbers: 75.50.Tt, 05.65.+b

Self-assembly, the spontaneous organization of materials into complex architectures on nano- and microscales, has many similarities with the classic phenomena of self-organization in nonequilibrium systems such as Rayleigh-Benard convection and induced chemical patterns [1]. Ordered and chaotic wave patterns on the surface of a fluid subjected to a vertical vibration (Faraday waves or crispations) are pivotal for the understanding of fluid instabilities [2]. Recently, analogues of Faraday waves have been discovered in a variety of systems, ranging from granular materials [3] to ferrofluids [4]. Experimental studies of the nonequilibrium self-organization of particles with long-range interactions (magnetic, hydrodynamic, electrostatic) revealed surprising phase transitions and patterns [5–10]. The formation of dense clusters and loose quasi-one-dimensional chains and rings was observed. Besides being of direct relevance to the physics of granular media and out-of-equilibrium pattern formation, these studies provide insight into the fundamental problem of dipolar hard sphere fluids, for which the nature of solid-liquid transitions is a subject of debate [11].

In this Letter, we report the discovery of snakelike self-assembled structures induced by an alternating (ac) magnetic field in an ensemble of magnetic microparticles placed at the liquid-air interface. We show that these structures are formed because of the interplay between surface waves on the liquid’s surface and the collective response of magnetic particles to an external ac magnetic field. The “snakes” possess unique magnetic structure: their segments exhibit long-range antiferromagnetic ordering, while each segment is composed of ferromagnetically aligned chains of microparticles. The generated structures exhibit magnetic hysteretic behavior with respect to an external in-plane magnetic field and a logarithmic relaxation of the magnetic moment. The generated multisegment structure can be fine-tuned by changing the frequency and amplitude of the magnetic field. The snakes generate large-scale fluid vortex motion and exhibit a variety of instabilities.

The experimental setup is shown in Fig. 1. Magnetic microspheres are suspended over the surface of water and supported by surface tension at the liquid-air interface. The

diameter of the container and the depth of the water are 50 mm. The particles are energized by a vertical ac magnetic field, H_{ac} , produced by a set of magnetic coils (170 mm in diameter) capable of creating fields up to 120 Oe. In addition, an in-plane dc magnetic field H_{dc} (up to 30 Oe) can be created with a pair of Helmholtz coils to probe the magnetic properties of the self-assembled structures. Spherical $\sim 90 \mu\text{m}$ (80–100 μm uniform size distribution) nickel particles were used in the experiment: the magnetic moment per particle in an 80 Oe external magnetic field is 1×10^{-5} emu; the corresponding saturated magnetic moment is 2×10^{-4} emu per particle at a saturation field of about 4 kOe. The inhomogeneity of the field in our setup is negligible: the magnetic force associated with the vertical field gradient per particle is less than 1% of its gravitational force.

Magnetic particles subjected to a uniform constant magnetic field experience a torque, forcing their magnetic moments to be aligned with the applied magnetic field [7]. As a consequence, the particles experience strong dipole-dipole repulsions from each other, resulting in the formation of a two-dimensional lattice structure on the surface of water [12,13]. In contrast, an alternating magnetic field creates a new nontrivial phenomenon. An astounding self-organized multisegment structure emerges as

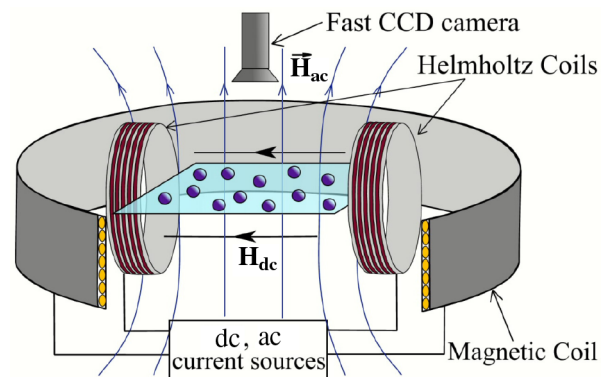


FIG. 1 (color online). Schematic view of the experimental setup.

a result of the collective interaction between the particles and the surface excitations; see Fig. 2.

Each segment of the snake structure consists of ferromagnetically aligned chains composed of particles whose magnetic moments are aligned along the chain direction. The chain formation is driven by magnetic dipole-dipole interactions, which govern the local arrangement of the magnetic particles [5,7]. The number of chains in a segment can be tuned by the frequency of the applied magnetic field: a low frequency drive results in an increase in the number of ferromagnetic chains in each segment; see Fig. 2. There is a critical amplitude of the driving force below which no structure is formed (see [14]). The generated snakelike structure is strongly hysteretic with respect to the ac field amplitude: it can be destroyed at high amplitude (by mechanical shaking) and the structure reappears only after the driving amplitude is decreased. Even though the number of chains in a segment can be tuned by the field amplitude—excitation at lower driving field amplitude generates more chains within each segment at a given frequency—the characteristic wave length of the structure is not affected. In contrast to the magnetic ordering within the segments, the orientation of the magnetic moments in the neighboring sections of the snake is anti-ferromagnetic, as shown below.

The excitation of surface waves by oscillating magnetic particles responding to an ac magnetic field is analogous to Faraday waves and is the primary mechanism for the formation of the snakes. In the course of aligning with the magnetic field, the particles drag the surrounding fluid and produce local oscillations of the water's surface, thereby affecting other particles. If the particles happen to be close enough to one another, the head-to-tail dipole-dipole attraction overcomes the repulsion favored by alignment of particles with the external field. As a consequence, a chain of particles is formed, with the resulting magnetic moment pointing along the chain. The chain produces wavelike local oscillations which facilitate the self-

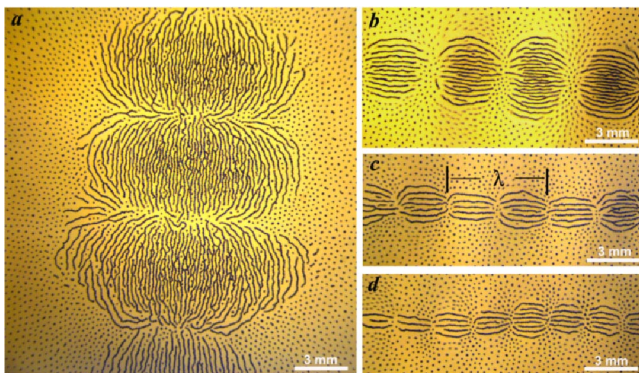


FIG. 2 (color online). Snake structures generated by a vertical ac 110 Oe magnetic field. The size of the segments is determined by the magnetic field frequency ν . Panel (a) corresponds to $\nu = 17$ Hz excitation; (b), (c), and (d) represent structures generated at 30, 50, and 70 Hz, respectively.

assembly process: a component of the magnetic field further promotes chaining of particles parallel to the wave's surface. A sketch of the coupling mechanism between chains and a surface wave is shown in the top panel of Fig. 3. In a round container, there is no preferred orientation for the snake structure. However, in a rectangular shaped container the directions parallel to the walls of the container are preferable for structure formation. As in Faraday's experiment, the characteristic dimension of the pattern is closely related to the parameters of the excited surface wave. However, in contrast to Faraday waves, the structures that appear in our experiment are always harmonic: they acquire the periodicity of the driving frequency. In the majority of Faraday-type experiments, the response is subharmonic. Figure 3 shows the full period of the snakes as a function of the external field frequency (see also Fig. 2).

The length scale of the snake closely follows the dispersion relation for surface waves in water, accounting for the surface tension and magnetic contribution [4,15]:

$$\nu^2 = \frac{g}{2\pi\lambda} + \frac{2\pi T}{\rho\lambda^3}(1 - \alpha). \quad (1)$$

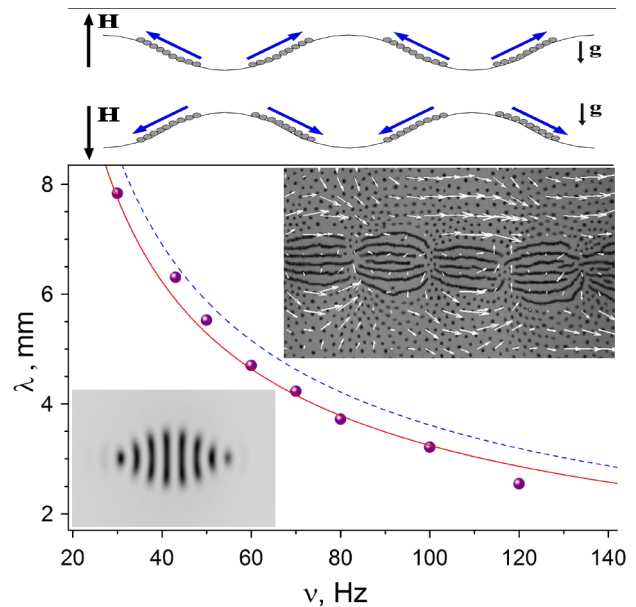


FIG. 3 (color online). Top panel: Sketch of the instability mechanism. Arrows indicate the orientation of the magnetic moment in the segments. Bottom panel: Characteristic length of the snake λ vs frequency ν . Symbols show experimental data for 110 Oe field amplitude. The dashed line represents the dispersion relation for surface waves in deep water (no fitting parameters). The solid line represents the dispersion relation for surface waves in water, accounting for the magnetic contribution [see Eq. (1)] with $\alpha = 0.28$. Top inset: Velocity field in the vicinity of the snake structure at $\nu = 50$ Hz. Bottom inset: Pattern obtained by numerical modeling. The intensity of the dark color is proportional to the density of the magnetic particles. Parameters in Eq. (2) are $\epsilon = 1$, $b = 2$, $\gamma = 2.5$, $D = 1$, $\beta = 8.5$, and $\omega = 3$, in the domain of 100×100 dimensionless units.

Here, ρ is the density of water, g is the gravitational acceleration, T denotes the water surface tension constant, and α is the effective magnetic contribution to the surface tension, which depends on the particle concentration and magnitude of the magnetic field. Apparently, α should be positive, since the magnetic dipole-dipole repulsion between particles introduces some “softening” of the surface.

A surprising new feature of our experiment is the generation of large-scale vortex flows in the vicinity of the snakelike structure (top inset of Fig. 3). The flow patterns visualized with the help of particle-image velocimetry are shown by arrows. Because of nonlinear effects, the snake creates rotating vortex flows despite the fact that the magnetic field is vertical (see also the supporting movies [14]). The flow can be as fast as 2 cm/s and depends on the magnetic field parameters. When the frequency of the magnetic field is increased, the stationary snake loses its stability (see [14]) and the entire structure begins to move erratically in the container.

The mechanism of parametrically driven surface waves in these experiments is similar to the one reported earlier for ferrofluids [16,17]. A major difference, however, is the fact that the dominant response of a ferrofluid to external vertical magnetic driving comes at half frequency, as does that found in vibrated water and sand layers (harmonic response was reported for the free surface of a ferrofluid driven with the parallel ac magnetic field [18]). Experiments on surface waves in ferrofluids are often performed in a static transverse magnetic field close to the critical field of a Rosensweig instability (both static and ac magnetic fields are collinear), making the system react differently to the up and down directions of the driving ac field. The situation is different when the magnetic particles and chains on the surface are driven solely with an ac magnetic field. As one can see from Fig. 3, nearly horizontal chains pull the surrounding fluid up (or down) at each driving cycle, resulting in a harmonic response of the induced standing waves.

The formation of the snake structure can be understood in the framework of an amplitude equation for parametric waves coupled to the conservation law describing the evolution of the magnetic particles density. We previously used a similar approach to describe self-localized structures (oscillons) in vibrating granular layers [19]. We describe our system with a set of two coupled equations:

$$\begin{aligned}\partial_t \psi &= -(1 - i\omega)\psi + (\varepsilon + ib)\nabla^2 \psi - |\psi|^2 \psi + \gamma \psi^* f(\rho), \\ \partial_t \rho &= D\nabla^2 \rho - \beta \nabla(\rho \nabla |\psi|^2).\end{aligned}\quad (2)$$

The first equation here is a paradigmatic model for parametrically excited surface waves (ψ is the complex amplitude of surface wave $\sim \psi \exp(i\omega t) + \text{c.c.}$, $\omega = 2\pi\nu$) that includes parametric driving $\gamma \psi^*$ (with $\gamma \propto H_0^2$) and nonlinear damping $|\psi|^2 \psi$. The linear operator in the equation for ψ is obtained by expansion of the dispersion relation Eq. (1) near the frequency ω and corresponding wave

number k (here $k \approx \sqrt{\omega/b}$), and $\varepsilon \nabla^2 \psi$ models viscous dissipation. The second equation expresses the conservation law for particle density ρ . Here, D is the diffusion coefficient and β is the amplitude of the advection term describing the concentration of particles by waves. The function f is proportional to ρ for small densities and saturates for larger densities. Without loss of generality, we took $f = \rho - 0.3\rho^2$. Equation (2) describes the formation of localized snakelike structures over a wide range of parameters. Contrary to the situation considered in Ref. [19], the self-localization occurs because surface oscillations can herd the magnetic particles into particular regions and reduce their concentration in neighboring areas. Since the magnitude of the driving force is proportional to the local particle concentration, surface wave excitation occurs only in the particle-rich areas (note that the model is not intended to reproduce the internal structure of the segments). A representative pattern is shown in Fig. 3.

As mentioned earlier, each segment consists of a set of ferromagnetically ordered parallel chainlike structures with the length controlled by the wavelength of the induced surface wave. The interchain distance within a segment is apparently determined by the repulsion of parallel dipole structures. The segments, however, are antiferromagnetically aligned: the total magnetic moment per segment reverses its direction from section to section. To demonstrate this, a small in-plane dc magnetic field was applied to the generated structure. The response of the snake to the in-plane dc magnetic field is illustrated in Fig. 4. A dc in-plane field applied perpendicular to the structure’s axis generates zigzag ordering of the segments indicative of the antiferromagnetic arrangement of the neighboring sections. Thus, the entire structure represents a multidomain magnetic object with short-range ferromagnetic ordering (within each segment) and long-range antiferromagnetic arrangement (between segments). It is apparent that the

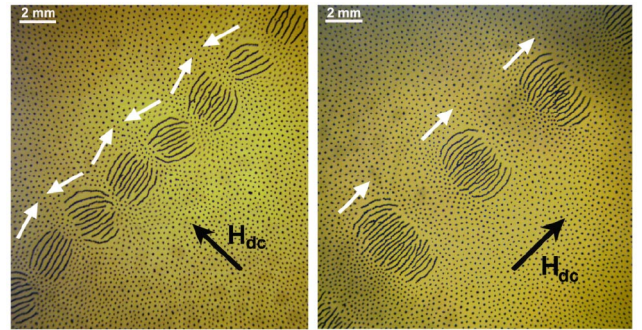


FIG. 4 (color online). Response of the snake to an in-plane magnetic field. The structure was generated by 50 Hz, 110 Oe driving field. White arrows designate directions of the magnetization vector at corresponding segments. Left panel: An in-plane dc magnetic field of 2 Oe was applied perpendicular to the structure. The resulting zigzag structure reflects the antiferromagnetic arrangement of the segments. Right panel: The in-plane dc field (10 Oe) was applied parallel to the snake structure.

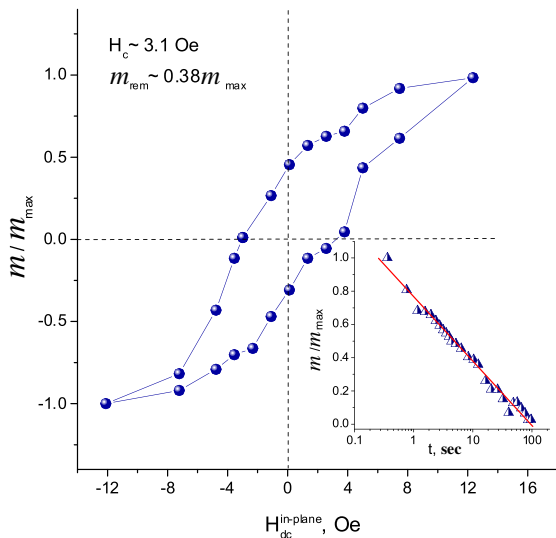


FIG. 5 (color online). Normalized M vs in-plane magnetic field for the snake generated with a 40 Hz, 110 Oe external magnetic field. M_{\max} corresponds to the effective magnetic moment at the 10 Oe in-plane dc field. At each point, the system was left to relax for 300 s after the in-plane magnetic field was changed. M is normalized to its maximal value M_{\max} . The corresponding coercivity force (H_c) is about 3.1 Oe. Inset: Relaxation of M from a single orientation state in a zero in-plane magnetic field (50 Hz, 110 Oe amplitude driving).

mechanism governing the antiferromagnetic arrangement of the segments comes from the induced surface wave, since pure magnetic dipole-dipole interactions would favor a parallel orientation of the segment's magnetic moments. A dc in-plane field applied parallel to the structure leads to a gradual decrease in the number of chains with antiparallel orientation of the magnetic moments. A snake with only one segment orientation is shown in Fig. 4 (right panel).

The magnetic ordering in our structures can be characterized by an effective moment M proportional to the product of the total length and number of chains in a segment. The effective “magnetization” is then defined as a sum over all segments. Defined in such a way, the effective magnetization of the structure exhibits hysteretic behavior with respect to the external static in-plane magnetic field, a typical feature of multidomain magnetic structures [20]. The hysteresis loop obtained for the snake generated with $\nu = 40$ Hz (110 Oe field amplitude) is demonstrated in Fig. 5. In addition, after being excited to a state with a single orientation of the segments by an in-plane field, the remanent effective magnetic moment relaxes logarithmically to its equilibrium state (see Fig. 5, inset). The process of effective magnetic moment relaxation proceeds mostly through the assembly of long chains out of single particles and shorter chains, and through the physical rotation of the chains towards a favorable magnetization direction. Logarithmic relaxation is well known

in magnetic materials [21], in a more general class of disordered systems, such as spin glass [22].

In conclusion, we studied the surface wave assisted formation of magnetic structures in an ensemble of suspended magnetic microparticles. We found that the excitation of the system by a vertical ac magnetic field results in the formation of multisegment, magnetic structures. Our experiment provides an attractive platform for modeling complex collective phenomena in a broad variety of systems, such as spin glasses, ferrofluids, and dense colloidal suspensions.

This research was supported by U.S. DOE, Grant No. W-31-109-ENG-38.

- [1] M. C. Cross and P. C. Hohenberg, *Rev. Mod. Phys.* **65**, 851 (1993).
- [2] A. Kudrolli and J. P. Gollub, *Physica (Amsterdam)* **97D**, 133 (1996).
- [3] P. Umbanhowar, F. Melo, and H. L. Swinney, *Nature (London)* **382**, 793 (1996).
- [4] R. E. Rosensweig, *Annu. Rev. Fluid Mech.* **19**, 437 (1987).
- [5] D. L. Blair and A. Kudrolli, *Phys. Rev. E* **67**, 021302 (2003).
- [6] J. Stambaugh *et al.*, *Phys. Rev. E* **68**, 026207 (2003); **70**, 031304 (2004).
- [7] A. Snezhko, I. S. Aranson, and W.-K. Kwok, *Phys. Rev. Lett.* **94**, 108002 (2005).
- [8] M. V. Sapozhnikov, Y. V. Tolmachev, I. S. Aranson, and W.-K. Kwok, *Phys. Rev. Lett.* **90**, 114301 (2003).
- [9] G. A. Voth *et al.*, *Phys. Rev. Lett.* **88**, 234301 (2002).
- [10] B. A. Grzybowski, H. A. Stone, and G. M. Whitesides, *Nature (London)* **405**, 1033 (2000).
- [11] P.-G. de Gennes and P. A. Pincus, *Phys. Kondens. Mater.* **11**, 189 (1970); Y. Levin, *Phys. Rev. Lett.* **83**, 1159 (1999); J. M. Tavares, J. J. Weis, and M. M. Telo da Gama, *Phys. Rev. E* **65**, 061201 (2002).
- [12] M. Golosovsky, Y. Saado, and D. Davidov, *Appl. Phys. Lett.* **75**, 4168 (1999).
- [13] W. Wen, L. Zhang, and P. Sheng, *Phys. Rev. Lett.* **85**, 5464 (2000).
- [14] See EPAPS Document No. E-PRLTAO-96-062609 for movies of the snake structure and formation. For more information on EPAPS, see <http://www.aip.org/pubservs/epaps.html>.
- [15] L. D. Landau and E. M. Lifshits, *Fluid Mechanics* (Pergamon Press, New York, 1987).
- [16] D. Raïtt and H. Riecke, *Phys. Rev. E* **55**, 5448 (1997).
- [17] T. Mahr and I. Rehberg, *Europhys. Lett.* **43**, 23 (1998).
- [18] J.-C. Bacri *et al.*, *Europhys. Lett.* **27**, 437 (1994); *Phys. Rev. E* **50**, 2712 (1994).
- [19] L. S. Tsimring and I. S. Aranson, *Phys. Rev. Lett.* **79**, 213 (1997).
- [20] A. H. Morrish, *The Physical Principles of Magnetism* (John Wiley and Sons, New York, 1965).
- [21] A. Hubert and R. Schafer, *Magnetic Domains* (Springer, New York, 1998).
- [22] W. Luo *et al.*, *Phys. Rev. Lett.* **67**, 2721 (1991).